DOI: 10.1002/chem.201000796

Fluorescent Probes for Pd^{2+} Detection by Allylidene–Hydrazone Ligands with Excellent Selectivity and Large Fluorescence Enhancement

Honglin Li, Jiangli Fan, Fengling Song, Hao Zhu, Jianjun Du, Shiguo Sun, and Xiaojun Peng*[a]

Abstract: Because palladium is widely used in various catalysts and converters, which results in a high level of contamination of water systems and the soil by residual palladium, there is an urgent need for Pd^{2+}-sensitive and -selective probes. Based on the special affinity of Pd^{2+} to conjugated double-bond ligands, two fluorescence probes (**RPd2** and **RPd3**) that contain conjugated allylidene-hydrazone ligands that link to colorless rhodamine-spirolactam have been developed. The results show that conjugated allylidene-hydrazones have a much better affinity toward Pd^{2+}, and consequently provide the probes with more acute color change and fluorescence enhancement (≈170-fold), and better selectivity over other metal ions (especially platinum-group elements, or PGEs) than the unconjugated allyl-hydrazine. With richer electron density and a more suitable stereo effect in the allylidene-hydrazone group, **RPd2** displays the best specificity toward Pd^{2+} and affords convenient detection by the naked eye. Its potential application for Pd^{2+}-contaminated water and soil-sample analysis is revealed by proof-of-concept experiments.

Keywords: affinity · environmental chemistry · fluorescent probes · palladium · rhodamine

Introduction

Currently, considerable attention has been focused on the design and synthesis of fluorescent probes for heavy- (and inner-) transition-metal (HTM) ions because of their significant importance in chemistry, cellular biology, and environmental science.[1] Since monitoring an increase in intensity from a low level of fluorescence is typically more reliable than monitoring a reduction in the fluorescence intensity of a highly fluorescent sample when changes in fluorescence are small,[2a] it is much more important and still a challenge to design "off/on" fluorescence probes for these ions with respect to the fact that they usually act as typical fluorescence quenchers.[2b–e] On the basis of the well-known spirolactam (nonfluorescent) to ring-open amide (fluorescent) equilibrium, rhodamine frameworks have been considered an ideal mode for the construction of the off-on systems that have frequently been utilized to design fluorescence-enhanced probes for Cu^{2+}, Pb^{2+}, Fe^{3+}, Cr^{3+}, Hg^{2+}, and Au^{+}/Au^{3+}.[3]

Palladium is one of the platinum-group elements (PGEs; they consist of Pd, Pt, Ru, Rh, Os, and Ir); it is widely used in various materials such as dental crowns, catalysts,[4] fuel cells, and jewelry. Pd-catalyzed reactions such as the Buchwald–Hartwig, Heck, Sonogashira, and Suzuki–Miyaura reactions represent powerful transformations for the synthesis of complex molecules[5] and have played an important role in pharmacy. However, their frequent and fruitful use can also result in a high level of residual palladium, which may result in the contamination of water systems and soil[6a] and therefore cause a health hazard.[6b–d] Governmental restrictions on the levels of residual heavy metals in end products are very strict. Therefore, palladium detection has attracted tremendous attention. The traditional methods include atomic absorption spectrometry (AAS), inductively coupled plasma atomic emission spectrometry (ICP-AES), solid-phase microextraction high-performance liquid chromatography (SPME-HPLC), X-ray fluorescence, and so on,[7] which all suffer from the high cost of instruments and their requirement of highly trained individuals.

[a] H. Li, J. Fan, F. Song, H. Zhu, J. Du, S. Sun, Prof. X. Peng
State Key Laboratory of Fine Chemicals
Dalian University of Technology, 158 Zhongshan Road
Dalian 116012 (P.R. China)
Fax: (+86) 411-39893800
E-mail: pengxj@dlut.edu.cn

Supporting information for this article is available on the WWW under http://dx.doi.org/10.1002/chem.201000796. It includes ^{1}H NMR and ^{13}C NMR spectra, absorption and fluorescence spectra, Pd^{2+} selective detection, S^{2-} titration, Job plots and pH effects for **RPd3**, detection-limit calculation, and charge numbers of atoms in ligands of **RPd2** and **RPd3**.

The fluorescence method has been developed for palladium analysis in recent years, although a colorimetric technique has frequently been applied.[8] For instance, palladium could be detected by fluorescent ligands through fluorescence quenching.[9] Holdt et al. designed the first chemosensor for Pd^{2+} detection by increasing fluorescence.[10a] In their system, they showed for the first time that oxidative photoinduced electron transfer (PET) in a molecular sensor of the fluorophore–spacer–receptor system can be regulated by the internal charge transfer (ICT) of a push/pull receptor.[10a,b] Recently, they have also reported the combination of a charge-transfer (CT) modulated PET with an excimer formation in an anthracenophane-type fluoroionophore for sensing Pd^{2+} by large fluorescence enhancement.[10c] Koide's group developed a fluorescein system as a sensitive (0.95–95 ng) and selective fluorescent sensor on the basis of Pd-catalyzed Tsuji–Trost[11] allylic oxidative insertion reaction, which displayed multiple advantages for the analysis of residual palladium in reactors and in real samples of drugs, rocks, and soils.[10d–f] The excellent work by Holdt and Koide et al. has encouraged us to introduce the allyl groups into the spirolactam ring of a rhodamine derivative and thus design a rhodamine-based Pd^{2+} probe (**RPd1** in Scheme 1)[10h] with good selectivity, high sensitivity, and notable fluorescence enhancement in Pd^{2+} and Pd^{0} detection.

However, Hg^{2+} poorly quenches the fluorescence enhancement of **RPd1** on Pd^{2+}, and Pt or other PGE ions always show some fluorescence response, which is still a common shortcoming in these kinds of probes. It is known that Pd^{2+} always shows more affinity to conjugated bonds (such as C=C−C=C) than single C=C bonds. The conjugation and electron density of the ligand might therefore be very important for Pd^{2+} recognition and influence both the sensitivity and the selectivity of Pd^{2+} over Hg^{2+} and other PGE ions, especially in the cases of rhodamine spirolactam ring-opening systems induced by Pd^{2+} complexation on the ligands. Hence, in this study, we use the allylidene-hydrazone (N=C−C=C) groups to increase conjugation over the previous allyl-hydrazine (N−C−C=C) group in **RPd1**, and adjust their electron density with a methyl group (electron-donating) in **RPd2** and bi-cyano groups (electron-withdrawing) in **RPd3**. The results show that these new ligands do indeed have different effects on the selectivity, sensitivity and the fluorescence quantum yields after coordination with Pd^{2+}. **RPd2** displays an excellent fluorescence response, even in the presence of Hg^{2+}, and shows good selectivity over other PGE ions.

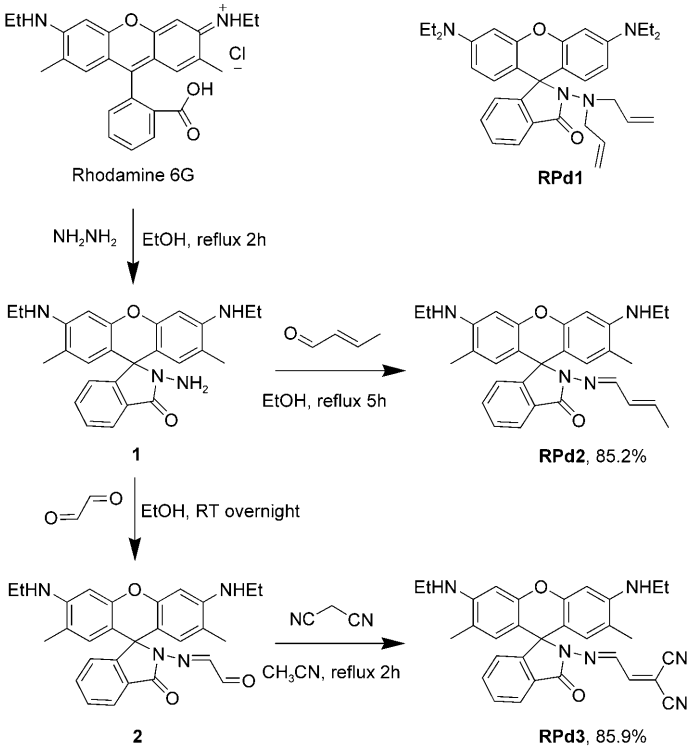

Scheme 1. Synthesis of **RPd1**, **RPd2**, and **RPd3**.

Results and Discussion

Synthesis and characterization of RPd2 and RPd3: **RPd2** was easily synthesized in 85.2% yield by a condensation reaction of rhodamine 6G hydrazide (**1**) and but-2-enal. **RPd3** was prepared in a similar yield (85.9%) by a condensation reaction of intermediate (**2**) and malononitrile (Scheme 1). The intermediates, **1** and **2**, were prepared according to procedures in the literature.[12] The structures of **RPd2** and **RPd3** were both confirmed by ^{1}H NMR and ^{13}C NMR spectra as well as time-of-flight mass spectrometry (TOF-MS) data.

Spectroscopic properties of RPd2 and RPd3: The free probes **RPd2** and **RPd3** are colorless and nonfluorescent because they are both in "ring-closed" states. After addition of Pd^{2+} to **RPd2** and **RPd3** solutions, the complexation induced the two probes to their "ring-open" states, thus leading to evident color change (from colorless to brilliant pink) and emission of a strong fluorescence. As displayed in Figure 1 as well as Figures S1 and S2 in the Supporting Information, in 50% ethanolic solution the absorption peaks of **RPd2**+Pd^{2+} and **RPd3**+Pd^{2+} center at 532 and 540 nm, respectively, and emission peaks both center at 555 nm. The fluorescence enhancement of **RPd2** (10 μM) to Pd^{2+} (1.0 equiv) is as high as 170-fold (Figure 1b). The colorimetric and fluorometric responses between the probes and Pd^{2+} can also be conveniently detected by the naked eye (Figure 2).

Pd^{2+} selectivities of RPd2 and RPd3 over other common cations: Achieving high selectivity toward the analyte of interest over other potentially competing species is a necessity for the fluorescence probe. The common cations such as K^{+}, Na^{+}, Ca^{2+}, Mg^{2+}, Zn^{2+}, Cd^{2+}, Ba^{2+}, Cr^{3+}, Pb^{2+}, Cu^{2+}, Hg^{2+}, Ag^{+}, Mn^{2+}, Ni^{2+}, Co^{2+}, La^{3+}, and NH_4^{+} (50 μM, respectively) were used to evaluate the metal-ion binding properties of **RPd2** (10 μM) in 50% ethanolic water solution.

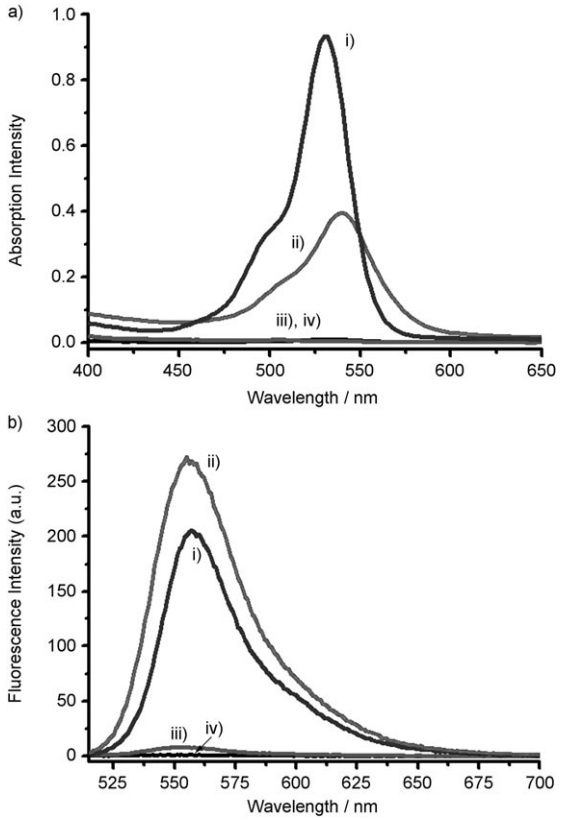

Figure 1. a) Absorption and b) fluorescence spectral changes of **RPd2** and **RPd3** before and after addition of Pd^{2+} (1.0 equiv) in 50% ethanolic water solution. 10 μM for **RPd2**, **RPd3**, and Pd^{2+}. Excitation wavelength is 505 nm. Slit: 5.0 nm/2.5 nm. i) **RPd2**+Pd^{2+}, ii) **RPd3**+Pd^{2+}, iii) **RPd3**, and iv) **RPd2**.

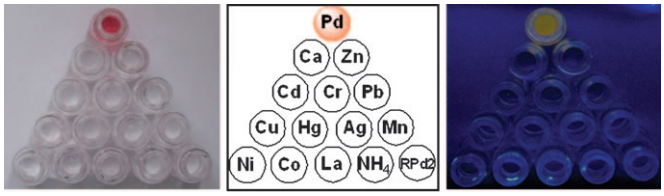

Figure 2. The colorimetric and fluorometric responses of **RPd2** to Pd^{2+} and other selected common cations in 50% ethanolic water solution, 30 μM for **RPd2** and Pd^{2+}, 50 μM for other cations. The two photos were obtained in sunlight (left) and upon excitation at 365 nm using a UV lamp (right), respectively. Pd = $PdCl_2$, Ca = $CaCl_2$, Zn = $Zn(NO_3)_2$, Cd = $CdCl_2$, Cr = $CrCl_3$, Pb = $Pb(NO_3)_2$, Cu = $Cu(NO_3)_2$, Hg = $HgCl_2$, Ag = $AgNO_3$, Mn = $MnCl_2$, Ni = $NiCl_2$, Co = $CoCl_2$, La = $LaCl_3$, and NH_4 = NH_4Cl; RPd2 represents the probe only.

The fluorescence spectra were obtained by excitation of the rhodamine 6G fluorophore at 505 nm. **RPd2** displays no fluorescence response to all these metal ions, except that Pd^{2+} induces a large fluorescence enhancement (Figure S3a in the Supporting Information). The selective recognition of Pd^{2+} can be detected by the naked eye both for colorimetric and fluorometric methods, as shown in Figure 2. Additionally, competition experiments were also checked for **RPd2**. In the presence of these competitive cations, Pd^{2+} still leads to a similar fluorescence intensity (Figure S3b), which indicates that the Pd^{2+} detection by **RPd2** has little interference from the common cations.

In the case of **RPd3**, the antijamming abilities (Figure S4b in the Supporting Information) toward Pb^{2+}, Mn^{2+}, Ag^{+}, and NH_4^{+} ions are not as good as that of **RPd2**, but it also displays moderate selectivity for Pd^{2+} (Figure S4a). Moreover, the serious fluorescence quenching of the **RPd1**-Pd^{2+} system[10h] by Hg^{2+} in the previous work has been overcome in the cases of both **RPd2** and **RPd3**. It should therefore result in the conjugated allylidene-hydrazone groups having a better affinity toward Pd^{2+} than the unconjugated allyl-hydrazine groups toward Hg^{2+}.

Pd^{2+} selectivities of RPd2 and RPd3 over other PGE ions: PGEs are widely used as efficient catalysts, which have similar chemical properties. Herein, the effective discrimination of PGE ions would be much more important for reclaiming the noble metal. In our study, $PdCl_2$, $PtCl_2$, $RhCl_3$, and $RuCl_3$ were adopted to check whether or not **RPd2** and **RPd3** could selectively detect the PGEs ions. Figure 3a shows the time course (0–60 min) of fluorescence intensities of **RPd2** treated with Pd^{2+}, Pt^{2+}, Rh^{3+}, and Ru^{3+}, respectively. It can be clearly observed that the selected PGE ions do not enhance the fluorescence intensity of **RPd2**, whereas

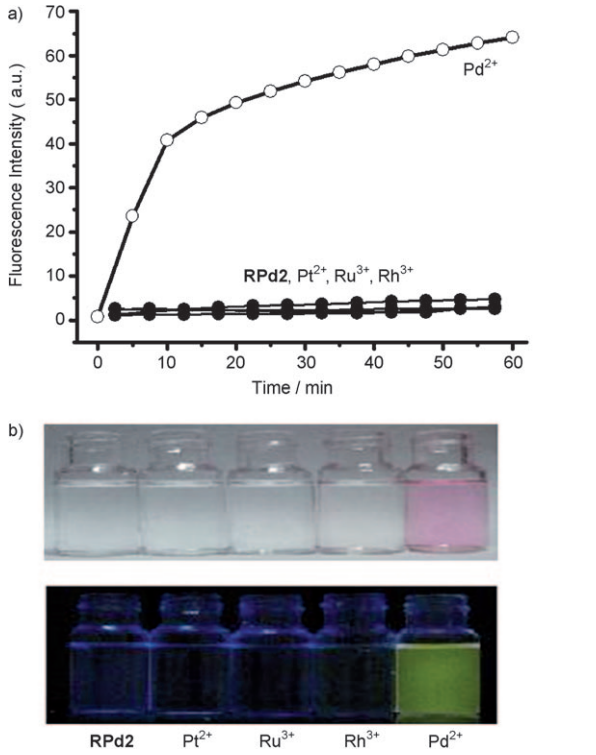

Figure 3. a) Time-dependent fluorescence intensity changes (at 555 nm) of **RPd2** (10 μM) with or without different PGE ions (1.0 equiv). Excitation wavelength is 505 nm, slit: 5.0 nm/2.5 nm. b) Visual absorption (top) and fluorescence (bottom) responses of **RPd2** (10 μM) with or without PGE ions (1.0 equiv) in 50% ethanolic water solution. The two photos were obtained in sunlight (top) and upon excitation at 365 nm using a UV lamp (bottom), respectively.

Pd^{2+} leads to a notable fluorescence signal, even after 10 h (Figure S7a in the Supporting Information). Similar results can be observed for **RPd3** (Figure S6 and S7b). To the best of our knowledge, this is the first report to obtain such excellent selectivity of a fluorescent probe toward Pd^{2+} in aqueous media over other PGE ions, especially Pt^{2+}.

The mechanism of Pd^{2+} detection by RPd2 and RPd3: In our previous work, **RPd1** displayed a good response to Pd^{2+} due to the well-known interaction between the allyl group and Pd^{2+}. In this study, we firstly used S^{2-} titrations of **RPd2**-Pd^{2+} and **RPd3**-Pd^{2+} systems to check the coordination between Pd^{2+} and the probes. When an excess amount of S^{2-} was added to the pink solutions of **RPd2**-Pd^{2+} and **RPd3**-Pd^{2+}, the solutions turned colorless and the fluorescence gradually disappeared (Figure 4a and Figure S8a in the Supporting Information), which should be attributed to the decoordination of Pd^{2+}. The Job plots show 2:1 stoichiometry between the probe and Pd^{2+} both for **RPd2** and **RPd3** in Figure 4b and Figure S8b. Another bit of evidence of the binding mode comes from TOF-MS spectra of the complex of **RPd2** and Pd^{2+}. The peak at m/z 533.2880 that corresponds to $[Pd(\mathbf{RPd2})_2]^{2+}$ (Figure 5) is clearly observed.

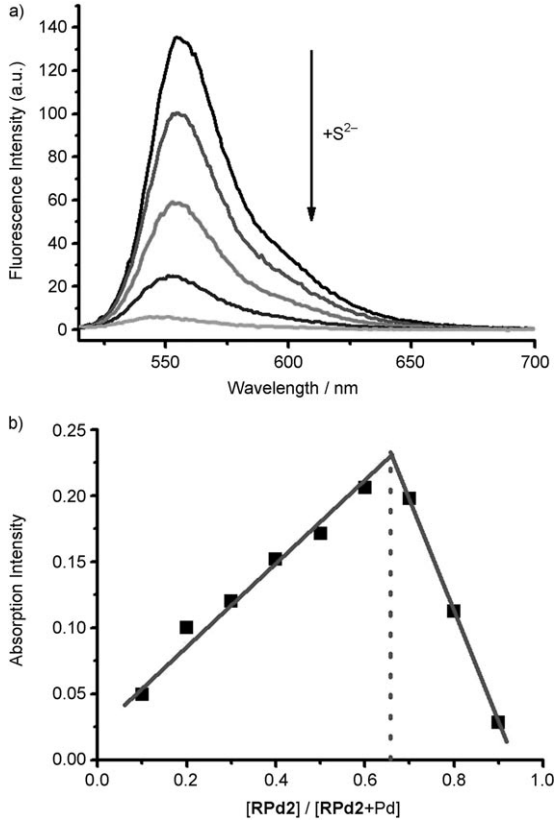

Figure 4. a) Fluorescence spectral changes of **RPd2**-Pd^{2+} solution (10 μM both for **RPd2** and Pd^{2+}) upon addition of an excess amount of S^{2-} ion in 50% ethanolic water solution. Excitation wavelength is 505 nm. Slit: 5.0 nm/2.5 nm. b) Job plots of **RPd2**. The total concentration of **RPd2** and Pd^{2+} is 10 μM.

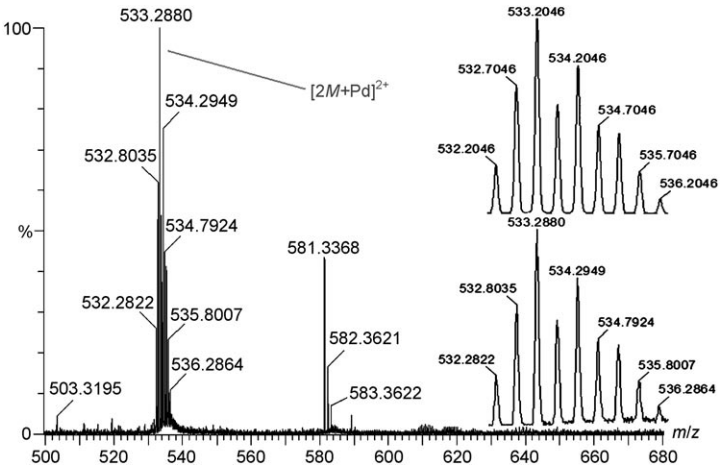

Figure 5. TOF-MS of **RPd2** (30 μM) in the presence of 1.0 equiv $PdCl_2$ in 50% ethanolic water solution. Insets: calculated (top) and observed (bottom) isotopic patterns for the $[Pd(\mathbf{RPd2})_2]^{2+}$ cation.

We think the conjugated Schiff base portion might be the key factor in the Pd^{2+}-sensing process, and the modified alkene groups have effectively adjusted in terms of electron density, coordinating properties, and stereo effect, which leads to the excellent selectivity of **RPd2** and **RPd3** toward Pd^{2+}. Bearing these in mind, the proposed mechanism is presented in Scheme 2: the spirolactam ring in the probes is opened by Pd^{2+} complexation.

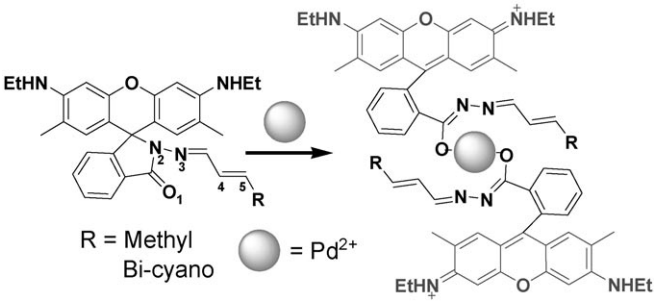

Scheme 2. Proposed mechanism for Pd^{2+} complexation inducing the opening of the spirolactam ring in **RPd2** and **RPd3**.

Effects of pH on probe emission and Pd^{2+} detection: The spirolactam ring of the rhodamine derivatives always opens in acidic media and indicates the fluorescence of rhodamine. It is therefore very important to check the fluorescence properties of **RPd2** and **RPd3** in solutions with different pH values. The acid–base titration control experiments were carried out by adjusting the pH with an aqueous solution of NaOH and HCl (Figure 6a and Figure S10a in the Supporting Information). The pH titration revealed that the probe solution did not emit any characteristic fluorescence at pH > 5. The resulting sigmoidal curves gave a similar pK_a of (3.41 ± 0.02) for **RPd2** and (3.42 ± 0.03) for **RPd3**, thus demonstrating that they can work in a wide pH range. The fluorescence responses of **RPd2** and **RPd3** in the absence and

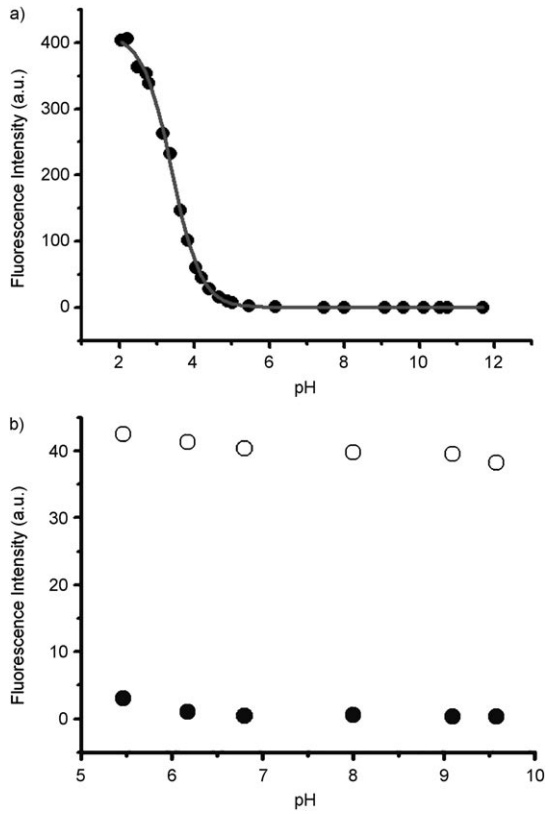

Figure 6. a) Effect of pH on the fluorescence intensity at 555 nm for **RPd2** (10 μM) in 50% ethanolic water solution. b) Pd^{2+} detection of **RPd2** in different pH. The pH of solution was adjusted by aqueous solution of NaOH (1 M) and HCl (1 M). Excitation wavelength is 505 nm. Slit: 2.5 nm/2.5 nm. ●: **RPd2**, ○: **RPd2** + Pd^{2+}.

presence of Pd^{2+} in different pH values were also evaluated. Figure 6b and Figure S10b display that, in near neutral pH range (5.46–9.58 for **RPd2** and 4.08–10.05 for **RPd3**), they can respond readily to Pd^{2+} without any interference by protons.

Different properties caused by different ligands in RPd2 and RPd3: With differing methyl and bi-cyano groups in each ligand on the spirolactam ring, **RPd2** and **RPd3** demonstrate different properties such as sensitivity and fluorescence quantum yield after coordination with Pd^{2+}.

The fluorescence intensities of **RPd2** and **RPd3** are both linearly proportional to the amount of Pd^{2+} added (0–1.0 ppm). As Figure S11a in the Supporting Information shows, **RPd2**, with a detection limit of 1.80×10^{-7} M (almost the same value as **RPd1**[10h]), is much more sensitive than **RPd3**, which has a detection limit of 1.70×10^{-6} M (Figure S11b). That is probably because **RPd2** (which contains an electron-donating methyl group) is relatively electron-richer than that of **RPd3** (which contains electron-withdrawing bi-cyano groups) at the allylidene-hydrazone part. This hypothesis is supported by the charge density of the atoms on the allylidene-hydrazone ligands of **RPd2** and **RPd3**, respectively (calculated by density functional theory (DFT) calculations at the B3LYP/6-31G level). The ligand that contains the methyl group in **RPd2** is much more electronegative than that of **RPd3**, which was clearly revealed by the charge on the O-1, N-2, N-3, and C-4 atoms in the allylidene-hydrazone part, as can be seen from Table 1 and Figure S12. Moreover, the different electronegativity is quite evident for C-5, which has a charge of −0.107 (negative value) in **RPd2** and a charge value of 0.140 (positive value) in **RPd3**. It suggests that electron-richer allylidene-hydrazones have a better affinity toward Pd^{2+}.

Table 1. The charge of atoms on the allylidene-hydrazone parts of **RPd2** and **RPd3** calculated by DFT methods (B3LYP/6-31G). For detailed information, see Figure S12 in the Supporting Information.

Atom	O-1	N-2	N-3	C-4	C-5
RPd2	−0.414	−0.519	−0.171	−0.098	−0.107
RPd3	−0.388	−0.503	−0.157	−0.054	0.140

As a heavy-metal ion, Pd^{2+} usually acts as a strong fluorescence quencher.[1a,2e,9,13] We have found that reduction of Pd^{2+} to Pd^0 would provide a much stronger fluorescence intensity in our previous work.[10h] In the present cases, it is interesting that the **RPd3**-Pd^{2+} system displays a higher fluorescence quantum yield than the **RPd2**-Pd^{2+} system ($\phi_{f3}/\phi_{f2}>$ twofold), which actually can be anticipated in Figure 1, from which we can see that the **RPd3**-Pd^{2+} system displays weaker absorption intensity but stronger fluorescence intensity. This is presumably because the quite different electron density caused by the substitutional groups has resulted in a discriminating fluorescence quenching effect from the Pd^{2+}-ligand complex to the rhodamine fluorophore in **RPd2**-Pd^{2+} and **RPd3**-Pd^{2+} systems, respectively. We think the electron-rich Pd(ligand-CH_3)$_2$ caused by a methyl group can facilitate the possible PET process to the excited rhodamine fluorophore, which has led to the partial fluorescence quenching effect. In the case of the **RPd3**-Pd^{2+} system, the bi-cyano group has made Pd(ligand-CN)$_2$ highly electron-deficient, which would effectively suppress the PET process to the excited fluorophore. It would result in a **RPd3**-Pd^{2+} system that has better fluorescence quantum yields than **RPd2**-Pd^{2+}.

Potential application of RPd2 for Pd^{2+} detection in water and soil samples: The potential utility of **RPd2** for Pd^{2+} detection was checked by proof-of-concept experiments. Pool and tap water were collected and filtered, prepared as 50% ethanolic water samples, and then spiked with different $PdCl_2$ ($[Pd^{2+}]_{final}=0$–10 μM) concentrations. The fluorescence signals of the water samples after the addition of **RPd2** solution ($[\mathbf{RPd2}]_{final}=10$ μM) were almost linearly correlated to the Pd^{2+} concentrations (Figure 7), which indicates that **RPd2** could be utilized for trace Pd^{2+} analysis in the pool- and tap-water samples. According to the test procedures for soil contamination in references,[10d,e] we found that fluorescence signals of Pd^{2+}-contaminated (>3 μM) soil samples after addition of **RPd2** (10 μM) evidently increased,

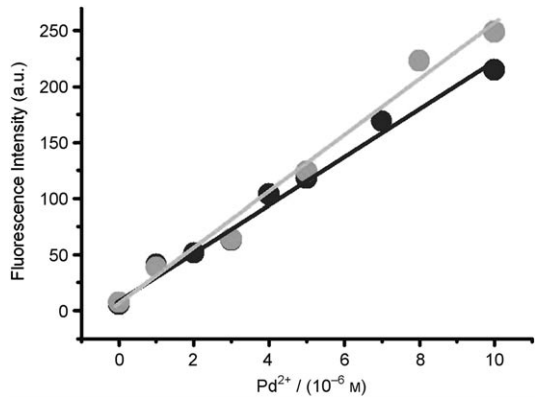

Figure 7. Proof-of-concept experiment with **RPd2** for Pd^{2+} detection in 50% ethanolic water (tap (●) and pool water (●)) solutions in μM levels. Excitation wavelength is 505 nm. Slit: 5.0 nm/5.0 nm.

thereby confirming its potential application for Pd^{2+} analysis in soil samples (Figure 8).[14]

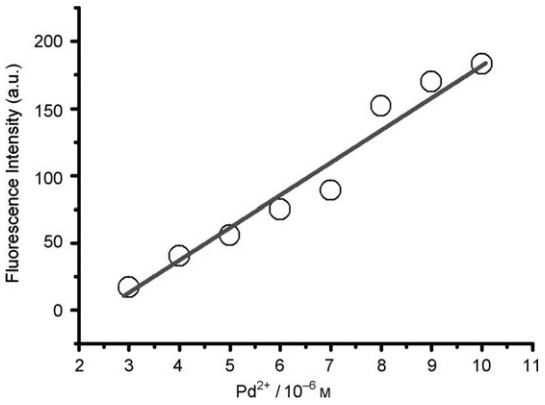

Figure 8. Proof-of-concept experiment with **RPd2** for Pd^{2+} detection in soil samples dissolved in 50% ethanolic water solution in μM levels. Excitation wavelength is 505 nm. Slit: 5.0 nm/5.0 nm.

Conclusion

In summary, we have developed two rhodamine-based fluorescence probes with conjugated allylidene-hydrazones, **RPd2** and **RPd3**. They have much better affinity toward Pd^{2+} and less interference from Hg^{2+} than previous unconjugated allyl-hydrazine (**RPd1**) and show excellent selectivity toward Pd^{2+} over other common cations and PGE ions. The colorimetric and fluorescent response to Pd^{2+} can be conveniently detected even by the naked eye, which provides a facile method for visual detection of Pd^{2+}. **RPd2** (with an electron-rich methyl groups in the allylidene-hydrazone ligand) displays better selectivity and sensitivity than **RPd3** (with electron-withdrawing bi-cyano groups). We also find that the highly electron-deficient system caused by the bi-cyano groups in **RPd3** can cause the **RPd3**-Pd^{2+} system to possess a relatively higher fluorescence quantum yield than the **RPd2**-Pd^{2+} system. Proof-of-concept experiments have also revealed the potential utilities of **RPd2** for Pd^{2+}-contaminated sample analysis.

Experimental Section

Materials and methods: All solvents used were of analytical grade. Analyte solutions were prepared from KCl, NaCl, NH_4Cl, $CaCl_2$, $BaCl_2{\cdot}2H_2O$, $MgCl_2{\cdot}6H_2O$, $CdCl_2{\cdot}2.5H_2O$, $CrCl_3{\cdot}6H_2O$, $MnCl_2{\cdot}5H_2O$, $NiCl_2{\cdot}6H_2O$, $CoCl_2{\cdot}6H_2O$, $Pb(NO_3)_2$, $LaCl_3{\cdot}7H_2O$, $AgNO_3$, $HgCl_2$, $Cu(NO_3)_2{\cdot}2.5H_2O$, $Zn(NO_3)_2{\cdot}6H_2O$, and $RuCl_3$ by separate dissolution in distilled water: 5.0 mM for $HgCl_2$, 10.0 mM for other cations. A 5.0 mM solution of $RhCl_3$ was prepared in an MeOH/H_2O (1:1 v/v) solution. A 5.0 mM solution of $PtCl_2$ was prepared in DMSO. A 5.0 mM stock solution of $PdCl_2$ (8.9 mg, 0.05 mmol) was prepared in 75:25 MeOH/brine (10 mL). Further dilution of the 5.0 mM stock solution of $PdCl_2$ with MeOH was carried out to prepare the 1.0 mM and 0.1 mM stock solutions. Solutions (10.0 mM) of **RPd2** (24.0 mg, 0.05 mmol) and **RPd3** (25.8 mg, 0.05 mmol) were both prepared in DMSO (5 mL) and stored in a refrigerator for use. ^1H and ^{13}C NMR spectra were recorded using a Varian INOVA-400 spectrometer with chemical shifts (δ) reported in ppm (in $CDCl_3$, TMS as internal standard). Mass spectrometry data were obtained using an HP1100 LC/MSD mass spectrometer and an LC/Q-TOF MS spectrometer. Fluorescence measurements were performed using a Varian CARY Eclipse fluorescence spectrophotometer (serial no. FL0812M018). All pH measurements were made using a Model PHS-3C meter.

Water-sample analysis by RPd2: The water samples (pool and tap water) were spiked with different $PdCl_2$ solutions ($[Pd]_{final}=0$–10.0 μM). Then equivalent ethanol was added, respectively, to prepare solutions in 50% ethanolic water solution. After filtering to remove insoluble materials, **RPd2** solution was added to the different Pd^{2+}-contaminated ethanolic water samples ($[\mathbf{RPd2}]_{final}=10.0$ μM).

Soil-sample analysis by RPd2: Soil was heated in an oven at 133 °C for 24 h prior to use. Then it was suspended in 50% ethanolic solution to prepare a 10.0 mg mL^{-1} soil sample and spiked with different $PdCl_2$ solutions ($[Pd]_{final}=0$–10.0 μM). After filtering to remove insoluble materials, **RPd2** solution was added to the different Pd^{2+}-contaminated soil samples ($[\mathbf{RPd2}]_{final}=10.0$ μM). Then fluorescence measurements were performed after equilibration.

Synthesis of RPd2: Compound **1** (500 mg, 1.2 mmol) was dissolved in ethanol (30 mL) in a 100 mL flask. But-2-enal (1 mL) was then added dropwise with vigorous stirring at reflux temperature for 5 h. After concentration to 10 mL, the solution was then cooled to room temperature. The resulting precipitate was filtered and washed three times with EtOH/water (15 mL). After drying over P_2O_5 under vacuum, the reaction afforded white **RPd2** (491.1 mg, yield: 85.2%). M.p. 302.3–303.1 °C; ^1H NMR (400 MHz, $CDCl_3$, 25 °C, TMS): $\delta=7.99$ (m, 1H; C_6H_4), 7.86 (d, $J=9.2$ Hz, 1H; NNCH), 7.41 (m, 2H; C_6H_4), 6.97 (m, 1H; C_6H_4), 6.38 (s, 2H; xanthene-H), 6.30 (s, 2H; xanthene-H), 6.12 (m, 1H; CH), 5.77 (m, 1H; CH), 3.52 (s, 2H; NH_2), 3.19 (q, $J=8.0$ Hz, 4H; CH_2), 1.88 (s, 6H; CH_3), 1.71 (d, $J=8.0$ Hz, 3H; CH_3), 1.31 ppm (t, $J=8.0$ Hz, 6H; CH_3); ^{13}C NMR (100 MHz, $CDCl_3$, 25 °C, TMS): $\delta=165.29$, 152.78, 150.89, 149.10, 147.41, 138.21, 133.33, 130.32, 127.88, 123.43, 118.15, 106.22, 96.93, 65.35, 38.45, 18.40, 16.70, 14.72 ppm; Q-TOF MS (ES^+): m/z: calcd: 481.2604 $[M+H]^+$; found: 481.2605.

Synthesis of RPd3: Compound **2** (500 mg, 1.1 mmol) was dissolved in acetonitrile (50 mL) in a 100 mL flask. Malononitrile (1 mL) was then added dropwise with vigorous stirring at reflux temperature for 2 h, and then the mixture cooled to room temperature. After removal of acetonitrile under vacuum, the residue was purified by flash chromatography with CH_2Cl_2/acetic ether as eluent to give **RPd3** as a red powder (443.8 mg, yield: 85.9%). M.p. 256.6–257.3 °C; ^1H NMR (400 MHz, $CDCl_3$, 25 °C, TMS): $\delta=8.17$ (m, 1H; $CHC(CN)_2$), 8.07 (d, $J=7.6$ Hz, 1H; C_6H_4), 7.58 (m, 2H; C_6H_4), 7.40 (d, $J=7.6$ Hz, 1H; NNCH), 7.09 (d, $J=7.6$ Hz, 1H; C_6H_4), 6.42 (s, 2H; xanthene-H), 6.19 (s, 1H; xanthene-H), 3.23 (q, $J=8.0$ Hz, 4H; CH_2), 1.89 (s, 6H; CH_3), 1.32 ppm (t, $J=$

8.0 Hz, 6H; CH_3); ^{13}C NMR (100 MHz, $CDCl_3$, 25 °C, TMS): δ = 166.00, 157.44, 152.48, 151.57, 148.28, 137.65, 135.59, 129.15, 127.64, 127.13, 124.52, 118.63, 112.85, 110.43, 109.07, 104.08, 96.95, 87.77, 67.08, 38.46, 16.85, 14.76, 8.80 ppm; Q-TOF MS (ES^+): m/z: calcd: 517.2352 $[M+H]^+$; found: 517.2330.

Fluorescence quantum yields: The fluorescence quantum yields of **RPd2**-Pd^{2+} and **RPd3**-Pd^{2+} were determined according to the method below [Eq. (1)]:

$$\varphi_u = \frac{(\varphi_s)(FA_u)(A_s)(\lambda_{exs})(\eta_u^2)}{(FA_s)(A_u)(\lambda_{exu})(\eta_s^2)} \quad (1)$$

in which ϕ is the fluorescence quantum yield; FA is the integrated area under the corrected emission spectra; A is the absorbance at the excitation wavelength; λ_{ex} is the excitation wavelength; η is the refractive index of the solution; and the subscripts u and s refer to the unknown and the standard, respectively. We chose rhodamine B as standard, which has a fluorescence quantum yield of 0.49 in ethanol.[15]

Theoretical calculations: The structures of **RPd2** and **RPd3** were optimized using density functional theory (DFT) by the B3LYP method with the 6-31G basis set. The DFT calculations were performed using the Gaussian 09 program.[16]

Acknowledgements

This work was supported by the NSF of China (20725621, 20706008, and 20923006), the National Basic Research Program of China (2009CB724706), the Ministry of Education of China (Program for Changjiang Scholars and Innovative Research Team in University, IRT0711; Cultivation Fund of the Key Scientific and Technical Innovation Project, 707016), and the Innovative Research Team of Liaoning Province (2006T026).

[1] a) A. P. de Silva, H. Q. Gunaratne, T. Gunnlaugsson, A. J.-M. Huxley, C. P. McCoy, J. T. Rademacher, T. E. Rice, *Chem. Rev.* **1997**, *97*, 1515–1566; b) F. P. Schmidtchen, M. Berger, *Chem. Rev.* **1997**, *97*, 1609–1646; c) R. Mártinez-Mánez, F. Sancenon, *Chem. Rev.* **2003**, *103*, 4419–4476; d) E. L. Que, D. W. Domaille, C. J. Chang, *Chem. Rev.* **2008**, *108*, 1517–1549; e) E. M. Nolan, S. J. Lippard, *Acc. Chem. Res.* **2009**, *42*, 193–203.

[2] a) F. Tanaka, N. Mase, C. F. Barbas III, *J. Am. Chem. Soc.* **2004**, *126*, 3692–3693; b) L. Fabbrizzi, M. Licchelli, P. Pallavicini, D. Sacchi, A. Taglietti, *Analyst* **1996**, *121*, 1763–1768; c) L. Prodi, F. Bolletta, M. Montalti, N. Zaccheroni, *Coord. Chem. Rev.* **2000**, *205*, 59–83; d) K. Rurack, *Spectrochim. Acta Part A* **2001**, *57*, 2161–2195; e) J. F. Callan, A. P. de Silva, D. C. Magri, *Tetrahedron* **2005**, *61*, 8551–8588.

[3] a) H. N. Kim, M. H. Lee, H. J. Kim, J. S. Kim, J. Y. Yoon, *Chem. Soc. Rev.* **2008**, *37*, 1465–1472; b) X. Q. Chen, S. W. Nam, M. Jou, Y. Kim, S. J. Kim, S. Park, J. Y. Yoon, *Org. Lett.* **2008**, *10*, 5235–5238; c) M. G. Yu, M. Shi, Z. G. Chen, F. Y. Li, X. X. Li, Y. H. Gao, J. Xu, H. Yang, Z. G. Zhou, T. Yi, C. H. Huang, *Chem. Eur. J.* **2008**, *14*, 6892–6900; d) X. L. Zhang, Y. Xiao, X. H. Qian, *Angew. Chem.* **2008**, *120*, 8145–8149; *Angew. Chem. Int. Ed.* **2008**, *47*, 8025–8029; e) Y. Zhou, F. Wang, Y. M. Kim, S. J. Kim, J. Y. Yoon, *Org. Lett.* **2009**, *11*, 4442–4445; f) A. Jana, J. S. Kim, H. S. Jung, P. K. Bharadwaj, *Chem. Commun.* **2009**, 4417–4419; g) A. Chatterjee, M. Santra, N. Y. Won, S. G. Kim, J. K. Kim, S. B. Kim, K. H. Ahn, *J. Am. Chem. Soc.* **2009**, *131*, 2040–2041; h) W. Huang, C. X. Song, C. He, G. J. Lv, X. Y. Hu, X. Zhu, C. Y. Duan, *Inorg. Chem.* **2009**, *48*, 5061–5072; i) J. H. Huang, Y. F. Xu, X. H. Qian, *J. Org. Chem.* **2009**, *74*, 2167–2170; j) M. J. Jou, X. Q. Chen, K. M. K. Swamy, H. N. Kim, H. J. Kim, S. G. Lee, J. Y. Yoon, *Chem. Commun.* **2009**, 7218–7220; k) Y. K. Yang, S. H. Lee, J. S. Tae, *Org. Lett.* **2009**, *11*, 5610–5613; l) O. A. Egorova, H. W. Seo, A. Chatterjee, K. H. Ahn, *Org. Lett.* **2010**, *12*, 401–403; m) J. J. Du, J. L. Fan, X. J. Peng, P. P. Sun, J. Y. Wang, H. L. Li, S. G. Sun, *Org. Lett.* **2010**, *12*, 476–479.

[4] a) J. Le Bars, U. Specht, J. S. Bradley, D. G. Blackmond, *Langmuir* **1999**, *15*, 7621–7625; b) T. Iwasawa, M. Tokunaga, Y. Obora, Y. Tsuji, *J. Am. Chem. Soc.* **2004**, *126*, 6554–6555; c) M. Lafrance, K. Fagnou, *J. Am. Chem. Soc.* **2006**, *128*, 16496–16497.

[5] a) G. Zeni, R. C. Larock, *Chem. Rev.* **2004**, *104*, 2285–2309; b) L. F. Tietze, H. Ila, H. P. Bell, *Chem. Rev.* **2004**, *104*, 3453–3516; c) K. C. Nicolaou, P. G. Bulger, D. Sarlah, *Angew. Chem.* **2005**, *117*, 4516–4563; *Angew. Chem. Int. Ed.* **2005**, *44*, 4442–4489; d) X. Chen, K. M. Engle, D. H. Wang, J. Q. Yu, *Angew. Chem.* **2009**, *121*, 5196–5217; *ngew. Chem. Int. Ed.* **2009**, *48*, 5094–5115.

[6] a) V. F. Hodge, M. O. Stallard, *Environ. Sci. Technol.* **1986**, *20*, 1058–1060; b) T. Z. Liu, S. D. Lee, R. S. Bhatnagar, *Toxicol. Lett.* **1979**, *4*, 469–473; c) J. C. Wataha, C. T. Hanks, *J. Oral Rehabil.* **1996**, *23*, 309–320; d) International Programme on Chemical Safety. Palladium; Environmental Health Criteria Series 226, World Health Organization, Geneva, **2002**.

[7] a) B. Dimitrova, K. Benkhedda, E. Ivanova, F. Adams, *J. Anal. At. Spectrom.* **2004**, *19*, 1394–1396; b) C. Locatelli, D. Melucci, G. Torsi, *Anal. Bioanal. Chem.* **2005**, *382*, 1567–1573; c) K. Van Meel, A. Smekens, M. Behets, P. Kazandjian, R. Van Grieken, *Anal. Chem.* **2007**, *79*, 6383–6389.

[8] a) P. Sarkar, P. K. Paria, S. K. Majumdar, *J. Indian Chem. Soc.* **1988**, *65*, 117–118; b) D. Kalný, A. M. Albrecht-Gary, J. Havel, *Anal. Chim. Acta* **2001**, *439*, 101–105; c) R. J. T. Houk, K. J. Wallace, H. S. Hewage, E. V. Anslyn, *Tetrahedron* **2008**, *64*, 8271–8278.

[9] a) E. Unterreitmaier, M. Schuster, *Anal. Chim. Acta* **1995**, *309*, 339–344; b) K. Kubo, Y. Miyazaki, K. Akutso, T. Sakurai, *Heterocycles* **1999**, *51*, 965–968; c) B. K. Pal, M. S. Rahman, *Mikrochim. Acta* **1999**, *131*, 139–144; d) Y. J. Fang, H. Chen, Z. X. Gao, X. Y. Jin, *Indian J. Chem. Sect. A* **2002**, *41*, 521–524; e) A. Tamayo, L. Escriche, J. Casabo, B. Covelo, C. Lodeiro, *Eur. J. Inorg. Chem.* **2006**, 2997–3004; f) J. R. Matthews, F. Goldoni, H. Kooijman, A. L. Spek, A. P. H. J. Schenning, E. W. Meijer, *Macromol. Rapid Commun.* **2007**, *28*, 1809–1815; g) L. P. Duan, Y. F. Xu, X. H. Qian, *Chem. Commun.* **2008**, 6339–6341.

[10] a) T. Schwarze, H. Müller, C. Dosche, T. Klamroth, W. Mickler, A. Kelling, H. G. Löhmannsröben, P. Saalfrank, H. J. Holdt, *Angew. Chem.* **2007**, 119, 1701–1704; *Angew. Chem. Int. Ed.* **2007**, *46*, 1671–1674; b) T. Schwarze, W. Mickler, C. Dosche, R. Flehr, T. Klamroth, H. G. Löhmannsröben, P. Saalfrank, H. J. Holdt, *Chem. Eur. J.* **2010**, *16*, 1819–1825; c) T. Schwarze, C. Dosche, R. Flehr, T. Klamroth, H. G. Löhmannsröben, P. Saalfrank, E. Cleve, H. J. Buschmann, H. J. Holdt, *Chem. Commun.* **2010**, *46*, 2034–2036; d) F. L. Song, A. L. Garner, K. Koide, *J. Am. Chem. Soc.* **2007**, *129*, 12354–12355; e) A. L. Garner, K. Koide, *Chem. Commun.* **2009**, 86–88; f) A. L. Garner, F. L. Song, K. Koide, *J. Am. Chem. Soc.* **2009**, *131*, 5163–5171; g) B. Tang, H. Zhang, Y. Wang, *Anal. Lett.* **2004**, *37*, 1219–1231; h) H. L. Li, J. L. Fan, J. J. Du, K. X. Guo, S. G. Sun, X. J. Liu, X. J. Peng, *Chem. Commun.* **2010**, *46*, 1079–1081.

[11] L. Kurti, B. Czako, *Strategic Applications of Named Reactions in Organic Synthesis*, Elsevier Academic Press, London, **2005**.

[12] a) X. F. Yang, X. Q. Guo, Y. B. Zhao, *Talanta* **2002**, *57*, 883–890; b) H. L. Li, J. L. Fan, J. Y. Wang, M. Z. Tian, J. J. Du, S. G. Sun, P. P. Sun, X. J. Peng, *Chem. Commun.* **2009**, 5904–5906.

[13] L. Fabbrizzi, M. Licchelli, P. Pallavicini, A. Perotti, A. Taglietti, D. Sacchi, *Chem. Eur. J.* **1996**, *2*, 75–82.

[14] The details for water and soil samples contaminated by Pd^{2+} are provided in the Experimental Section.

[15] K. G. Casey, E. L. Quitevis, *J. Phys. Chem.* **1988**, *92*, 6590–6594.

[16] Gaussian 09, Revision A.02, M. J. Frisch, G. W. Trucks, H. B. Schlegel, G. E. Scuseria, M. A. Robb, J. R. Cheeseman, G. Scalmani, V. Barone, B. Mennucci, G. A. Petersson, H. Nakatsuji, M. Caricato, X. Li, H. P. Hratchian, A. F. Izmaylov, J. Bloino, G. Zheng, J. L. Sonnenberg, M. Hada, M. Ehara, K. Toyota, R. Fukuda, J. Hasegawa, M. Ishida, T. Nakajima, Y. Honda, O. Kitao, H. Nakai, T. Vreven, J. A. Montgomery, Jr., J. E. Peralta, F. Ogliaro, M. Bearpark, J. J. Heyd, E. Brothers, K. N. Kudin, V. N. Staroverov, R. Kobayashi, J.

Normand, K. Raghavachari, A. Rendell, J. C. Burant, S. S. Iyengar, J. Tomasi, M. Cossi, N. Rega, J. M. Millam, M. Klene, J. E. Knox, J. B. Cross, V. Bakken, C. Adamo, J. Jaramillo, R. Gomperts, R. E. Stratmann, O. Yazyev, A. J. Austin, R. Cammi, C. Pomelli, J. W. Ochterski, R. L. Martin, K. Morokuma, V. G. Zakrzewski, G. A. Voth, P. Salvador, J. J. Dannenberg, S. Dapprich, A. D. Daniels, O. Farkas, J. B. Foresman, J. V. Ortiz, J. Cioslowski, and D. J. Fox, Gaussian, Inc., Wallingford CT, **2009**.

Received: March 30, 2010
Published online: September 17, 2010

